Long-range Correlations, MHD Effects, and Saw-tooth Oscillations in TCABR Biasing and Alfvén Heating Experiments

Yu.K. Kuznetsov 1), A.G. Elfimov 1), R.M.O. Galvão 2), I.C. Nascimento, 1) C. Silva 2), H. Figueiredo 2), L.F. Ruchko 1), J.H.F. Severo 1). I.L. Caldas 1), D.L. Toufen 1), Z.O. Guimarães-Filho 1), I. L., M. Machida 3), ,W.P. De Sá 1), J. I. Elizondo 1), E. Sanada 1), A.P. Reis 1), M.P. Gryaznevich 5), A.V. Melnikov 6), P. Duarte 3), F.O. Borges 1), T.M. Germano 1), O.C. Usuriaga 1), R. Arvin 8), V. Bellintani 12), G.P. Canal 4), R.M. de Castro 11), M. Ghoranneviss 8), M. Mizintseva 9), S. Mohammadi 8), V.E. Moiseenko 10), R. Narayanan 11), F. do Nascimento 3), M. Peres Alonso 2), G. Ronchi 3), L.M.F. Schmutzler 3), S.R.S. Tekieh 8), D.J. Trembach 7), G. Vorobyov 9)

1) Institute of Physics, University of São Paulo São Paulo, Brazil
2) Institute of Plasmas and Nuclear Fusion, Lisbon, Portugal
3) Institute of Physics, University of Campinas, Campinas, Brazil
4) Brazilian Center for Research in Physics, Rio de Janeiro, Brazil
5) EURATOM/UKAEA Fusion Association, Culham SC, Abingdon, UK
6) Institute of Nuclear Fusion, RRC "Kurchatov Institute", 123182, Moscow, Russia
7) Plasma Physics Laboratory, University of Saskatchewan, Canada
8) Plasma Physics Research Center, Islamic Azad University, Iran
9) Faculty of Applied Mathematics and Control Processes, Saint-Petersburg State University, Russia
10) NSC Kharkov Institute of Physics and Technology, Ukraine
11) Plasma Associate Laboratory, National Institute for Space Research, Brazil
12) Faculty of Technology of São Paulo, Brazil

E-mail: yuk@if.usp.br

Abstract. Long-distance correlations (LDC) of floating plasma potential fluctuations measured by an array of multi-pin Langmuir probes in the plasma edge have been investigated in TCABR experiments of small power Alfvén heating and external biasing H-mode. Experimental data confirm the effect of strong amplification of LDC in the potential fluctuations by biasing, recently observed in other experiments, whereas correlation of the density fluctuations is low. The frequency-wave number power cross spectrum of fluctuations is concentrated in the low frequency range $f < 50$ kHz, accumulating for $f < 5$ kHz (zonal flow) and with isolated maxima at $f \sim 15$ kHz (effect of MHD instability) and $f \sim 40$ kHz. The effects of the MHD activity on the LDC and on the sawtooth oscillations in Alfvén heating experiment are also investigated.

1. Introduction

One important issue related to zonal flows (ZFs) is the long distance correlation (LDC) of potential and density fluctuations along the equilibrium magnetic field lines. Recent results obtained in edge polarization experiments carried out on the TJ-II stellarator and on the ISTTOK and TEXTOR tokamaks indicate that while the correlation length of floating potential fluctuations can be of the order of the length of the plasma column, the density fluctuations show almost no correlation [1-4]. These highly correlated potential fluctuations have vanishing poloidal and toroidal wave numbers, $m \sim n \sim 0$, as predicted for zonal flows. Similar experiments carried out on the TJ-K stellarator have observed LDC also in the density fluctuations [5]. Actually, from a theoretical point of view, one expects that the potential fluctuations corresponding to zonal flows (ZF) to be of quite low frequency and to have no associated density fluctuations, whereas the ones associated with the geodesic acoustic modes

(GAMs) should have frequency $f_{GAM} \approx 5 \times [T_e/10\text{eV}]^{1/2}/R$ kHz and associated density fluctuations with $m = 1$ poloidal variation [6]. In this approximate expression for f_{GAM}, valid only for tokamaks close to the plasma edge, T_e is the electron temperature and R the major radius of the plasma column. An important question that has to be fully investigated and taken into consideration when comparing LDC measurements in stellarators and tokamaks is how they are affected by the presence of MHD activity, what essentially means investigating the interaction of saturated rotating islands with ZFs.

Another question that remains to be properly elucidated in tokamak physics is impurity accumulation in low density Alfvén heating experiments. Since the pioneering investigations carried out on TCA in Lausanne [7], this effect has remained a major hinder for high power Alfvén wave heating experiments in tokamaks.

In this paper we present results obtained in experiments carried out on the TCABR tokamak ($a = 0.18$ m, $R = 0.615$ m, $B_t = 1.1$ T) to investigate these questions as part of an experimental campaign organized within the framework of the *IAEA Coordinated Research Project on "Joint Experiments Using Small Tokamaks"* (May 2009).

2. Experimental Setup and Typical Discharges

In these experiments, the plasma current was kept within the range $I_p = 80\text{-}85$ kA and the line averaged plasma density was adjusted at $\bar{n} \approx 1.0\text{-}1.2 \times 10^{19}$ m^{-3}. The external electrostatic polarization was applied through a graphite electrode (8 mm high, 20 mm diameter) inserted vertically 10 mm into the edge plasma, at the bottom of the plasma column The floating potential and density fluctuations were measured with three multi-pin Langmuir probe arrays: a 6-pin forked probe, 5-pin probe, and 20-pin rake probe.

In some discharges, a small power (20-30 kW) Alfvén wave heating pulse was applied before or without the application of the external bias. This causes small electron heating $\Delta T_e \approx 30\text{-}50\text{eV}$, approximately 10% of the average electron temperature as measured by the ECE radiometer and Thomson scattering systems [8]. Two antenna modules separated by 180^0 in the toroidal direction were employed, exciting the $m/n = 1/2$ basic mode [9] appropriate for AW heating. To avoid a too large density increase during the application of the RF pulse, the gas puffing system is pre-programmed, decreasing slightly the gas inflow. Even though, impurity accumulation was detected through its influence on the sawtooth oscillations observed in central SXR channels, as discussed in the sequel.

The time evolutions of plasma current, plasma density, H-alpha emission, and MHD activity are presented in Fig 1 for two typical discharges of the experiments with external biasing. For the parameters of TCABR and plasma current in the range $I_p = 80\text{-}85$ kA, the 3/1 rational magnetic surface is located close to the plasma boundary, $r = 16 - 18$ cm, and frequently the 2/1 MHD mode tearing mode is triggered, as shown in Fig. 1. This mode generates a 3/1 magnetic island, due to toroidal coupling, which can be large enough to destroy the transport barrier [10,11]. In discharge 24126, the strong MHD mode appeared before biasing. In discharge 24128 the MHD instability was initially absent but was subsequently triggered during the electrostatic biasing. To keep the MHD activity somewhat under control and avoid disruptions, the electrode voltage was kept at value lower than in previous experiments [10,11]. With these parameters, the density increases up to $1.6\text{-}1.8 \times 10^{19}$ m^{-3}.
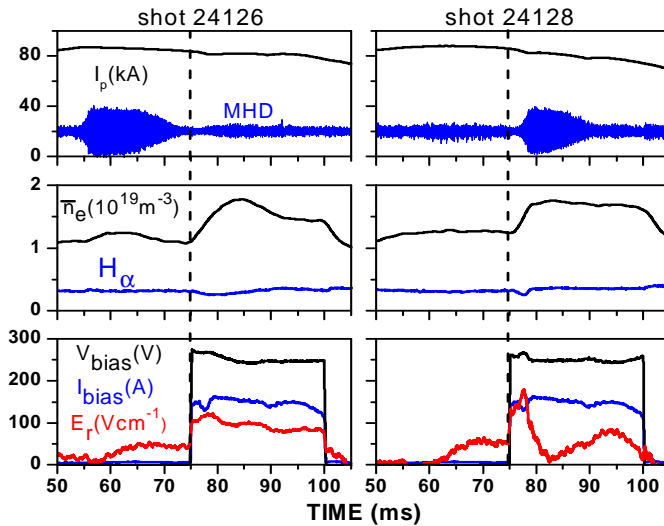
*FIG. 1. Discharge waveforms
with electrode biasing*

3. Analysis of Edge Fluctuations

The signals corresponding to the floating potential V_f and ion saturation current measured by the probes were acquired with a 2 MHz sampling rate. The cross-correlation between two signals (x and y) is defined as

$$C_{xy} = \left\langle [x(t+\tau) - \bar{x}][y(t) - \bar{y}] \right\rangle / \sqrt{\left\langle [x(t) - \bar{x}]^2 \right\rangle \left\langle [y(t) - \bar{y}]^2 \right\rangle^2},$$

where τ is the time lag. The time evolutions of C_{xy} are shown in Fig. 2 for both discharges. Here the same pin was chosen as the reference one. The poloidal distance between probes located at different toroidal positions is defined as the distance between second probe and magnetic line started at the reference probe. Let us first consider the cross-correlation between two pins located the same poloidal cross section and separated 0.4 cm in the poloidal direction; this is indicated by curves (a) in Fig 2. The correlation is quite high, 0.85 to 0.99 during the entire period of measurement. Curves (b) correspond to pins located in the same poloidal cross-section separated 0.5 cm radially. The value of the correlation decreases to a
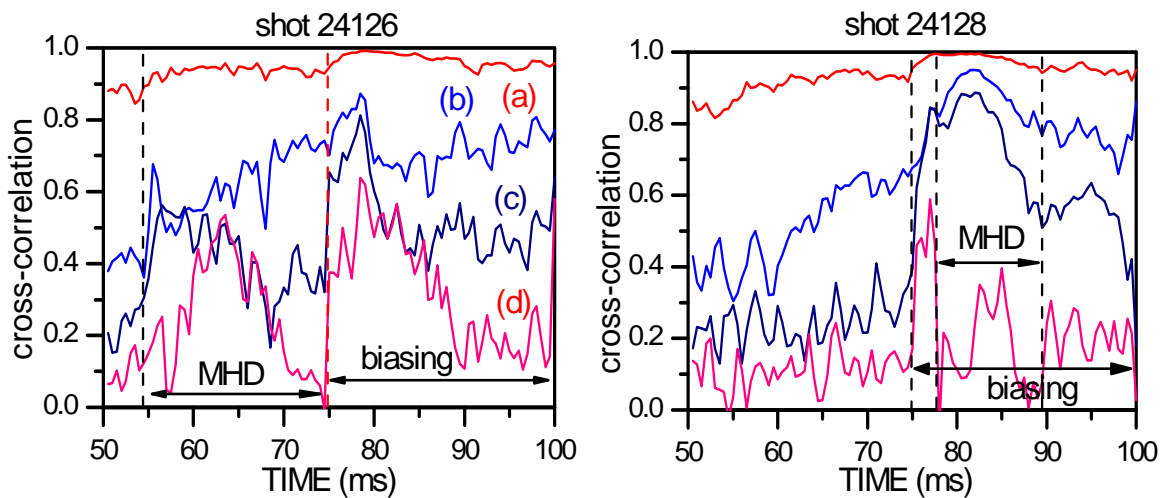

FIG. 2. Time evolution of cross-correlations between different probes for shots 24126 and 24128. Vertical dashed lines indicate time interval of high MHD activity and biasing (75 - 100 ms).

0.4 - 0.9, in both discharges. This smaller value of the radial correlation is expected for both ZFs and GAMs, which have finite radial wave number.

The LDCs are evidenced in the other two curves of Fig. 2. They correspond to various separation between pins: 56 cm in toroidal direction and 2.5 cm in poloidal direction (c) and 2.2 m in toroidal direction and 14 cm in poloidal direction (d). One can see significant LDC of ~ 0.2-0.4 already in the ohmic phase. With biasing, the correlation increases strongly both for short and long poloidal and toroidal distances and also for radial distance (b). For the case of mild separation in the toroidal direction, i.e., curve (c), the correlation increases with the appearance the MHD activity, in discharge 24126, before the biasing phase. Clearly this is just an effect of the edge MHD fluctuations associated with the 3/1 island. The correlation also increases substantially during the first 5-10 ms of the biasing phase and later saturates and starts to decrease. That the increase in the biasing phase has a different nature from the one associated with the MHD activity becomes evident from the analysis of the amplitude and cross-correlation spectra carried out in the sequel. Actually, when the MHD activity appears after biasing, its effect is always to reduce or quench the LDC amplified by biasing. This is more clearly shown for curves (c) and (d) for discharge 24128; they all rise sharply during the first 2-3 ms of the biasing phase, but the increase for the correlation between the probes separated in 2.2 m reduces sharply as the MHD activity sets in.

Cross-power spectrum provides information on the contribution of different spectral components to the correlation. The amplitude spectra and cross-spectra of oscillations in ohmic ($t = 60$-75 ms) and biasing ($t = 75$-90 ms) phases are shown in Fig. 3. The important experimental fact is appearance with biasing of highly coherent fluctuations with very low frequencies $f < 5$ kHz. In spite of low level of magnetic fluctuations measured by Mirnov probes, $\tilde{B}_p = 2 - 3 \times 10^{-3} B_{p0}$ in the biasing phase of shot 24126, there is the peak of amplitude at the frequency of 10-15 kHz close to that of the MHD during the ohmic phase. The same peak also occurs in spectra and cross-spectra of V_f. The third rather smooth maximum of amplitude is observed reproducibly in the biasing H-mode at the $f \sim 40$ kHz. The coherence spectrum defined as normalized cross-spectrum $\gamma_{12} = |S_{12}(f)| / \sqrt{S_1(f)S_2(f)}$, where S_{12} is (complex) cross-spectrum and S_1 and S_2 are the autopower spectra, is presented in Fig. 4. One can see that coherence decreases strongly with distance in the ohmic phase. The coherence increases with biasing. In the case of long distances, it is significant for frequencies below 60 kHz and increases strongly for very low frequencies $f < 5$ kHz.
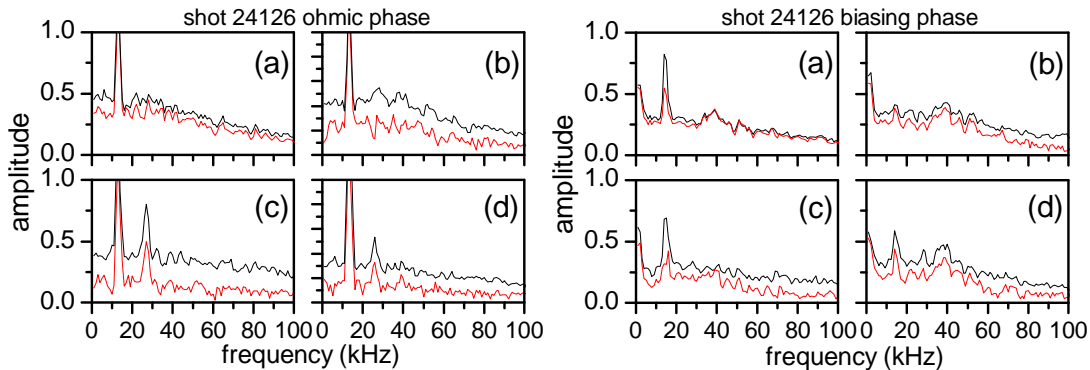

FIG. 3. Amplitude spectra (black) and cross-spectra (red) in ohmic and biasing phases for different distances from reference probe: d_rad = 5 mm (a); d_pol = 2.5 cm and d_tor = 56 cm (b); d_rad = 5 mm, d_pol = 14 cm and d_tor = 2.2 m (c); d_pol = 14 cm and d_tor = 2.2 m (d).
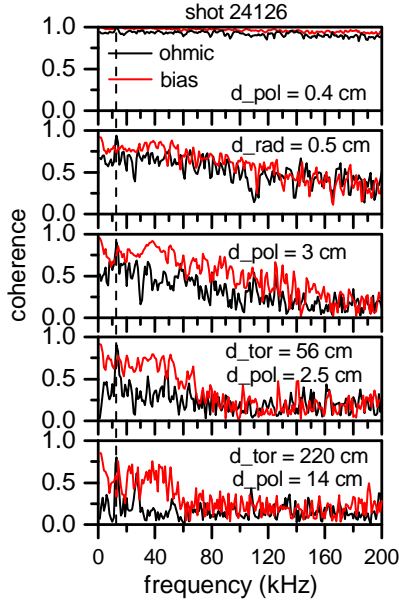
FIG. 4. *Coherence spectrum.*

More detailed information on the LDC properties can be obtained from the wavenumber-frequency spectrum $S(k,f)$ by a standard two-point technique. The local spectra calculated with short poloidal distance 0.4 cm between probes located at plasma edge in 0.5 cm from the limiter show that turbulent broadening in k decreases substantially and the autopower spectrum in wavenumber space $S(k)$ has maximum value at $k \sim 0$ with biasing (Fig. 5). For long distances between probes, the cross-spectrum $|S_{12}(k,f)|$ was calculated assuming sufficiently small wave numbers present in data (Fig. 6). For the distance of 220 cm in the toroidal direction, the maximum amplitudes at $\sim$ 15 kHz and $\sim$ 40 kHz occur with $|k| \sim 0.004$. The estimation of the poloidal and toroidal mode numbers as $m = rk$, $n = Rk$, gives $(m,n) \leq 0.3$.
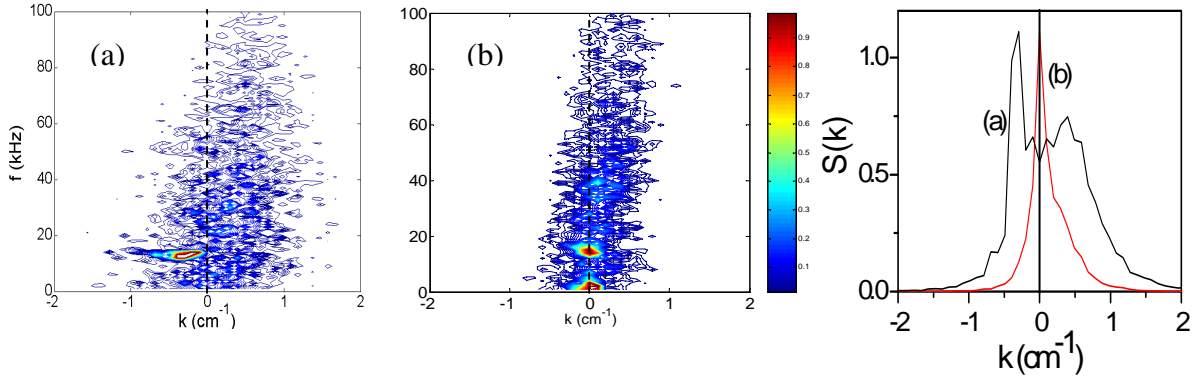

FIG. 5. *Local wavenumber-frequency power spectrum S (k,f) and power spectrum in wave number space S (k) for ohmic (a) and biasing (b) phases.*
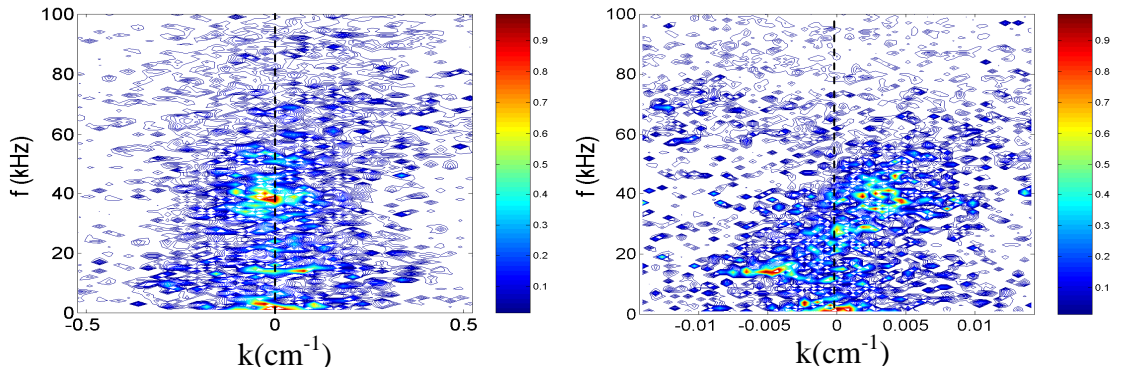

FIG. 6. *Wavenumber-frequency cross-spectrum S_{12} (k,f) for poloidal distance 3 cm (left) and toroidal distance 220 cm (right).*

4. Impurity and MHD instability effect on saw-tooth oscillation during AW heating

In TCABR standard ohmic discharge 23987 shown in Fig. 6 (similar to discharge 24126 before biasing), a regime with the sawtooth (ST) oscillations establishes when the ohmic current is about I≈80-90 kA. The ST oscillations are detected with ECE heterodyne and soft X-ray (SXR) emission from different cords viewing the plasma cross section, which signal is
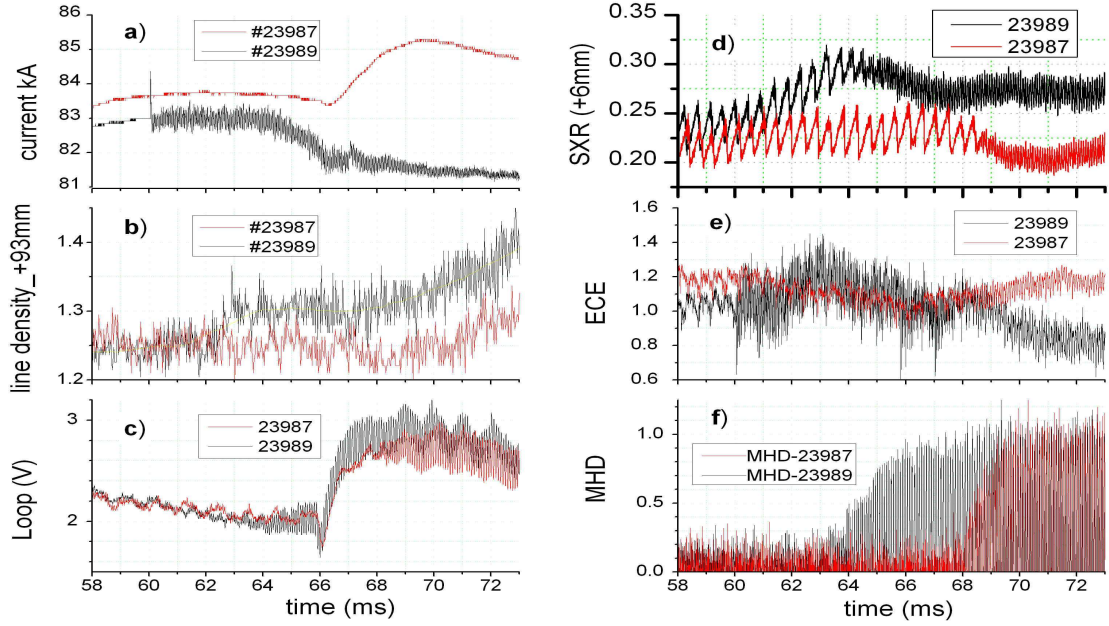
Fig. 7. Discharge waveforms of 23987 and 23989, current (a), density (b), loop voltage (c), core SXR signal (d), core ECE (e), and Mirnov oscillations (f).

proportional to Z_{ef} (effective plasma charge), what helps to clarify the impurity behavior in the plasmas. Detection of the saw tooth inversion radius with SXR at $r_{in} \approx 4\text{-}5\text{cm}$ helps in the identification of the $q=1$ surface and, therefore, the approximate plasma current distribution. This typical ST regime suddenly disappears during 3-4 intermediate oscillations after a small increase in the loop voltage at $t=0.066\text{s}$ shown in Fig. 7(a-c) for discharge 23987, which is externally applied to maintain the plasma current in TCABR. Then it is replaced by a regime with strong Mirnov oscillations accompanied by increasing impurity emission detected by SXR and optical spectroscopy. This sudden overshot of Mirnov oscillations with frequency, reduced from 16 to 12.5 kHz as shown in Fig. 7(d-e) and Fig. 8, is nonlinearly coupled with 5kHz oscillations as a prolongation of the old ST oscillations in the period 0.055-0.073 s.

The same effect is usually observed in a small power $P_A \approx 30$ kW Alfvén wave heating pulse, which is applied at $t = 0.06$ s during the discharge 23989 shown in Fig. 7, with the similar initial characteristics as discharges 2987 and 24126. The AW pulse produces small electron heating $\Delta T_e \approx 30\text{-}50\text{eV}$ detected by ECE emission, which is accompanied by increasing line-averaged density, CIII and CV lines and Soft X-ray emission, indicating impurity accumulation with Z_{ef} increasing of 10% in the plasma core. In Fig. 7 and Fig. 8, strong MHD oscillations with $m = 2$ appear with time delay about 3-4 ms after the AW application, as well as the ones appear at t=0.066s in the discharge 23987 and at t=0.054s in the discharge 24126 before biasing discussed in previous section. The MHD burst is accompanied by strongly growing SXR emission from the plasma core and diminishing amplitude of the ST oscillations. Finally, the ST oscillations disappear after 3-5 oscillations, indicating flattening of the electron temperature and current profiles and strong stable tearing mode island. The frequency of $m = n = 2$ island ($\omega = m\omega_i^* + nV/R_0$) is mainly attributed to the toroidal plasma rotation ($V \approx 22\text{-}28$ km/s) because the ion drift frequency is rather small, $f_i^* \approx 1.5$ kHz.
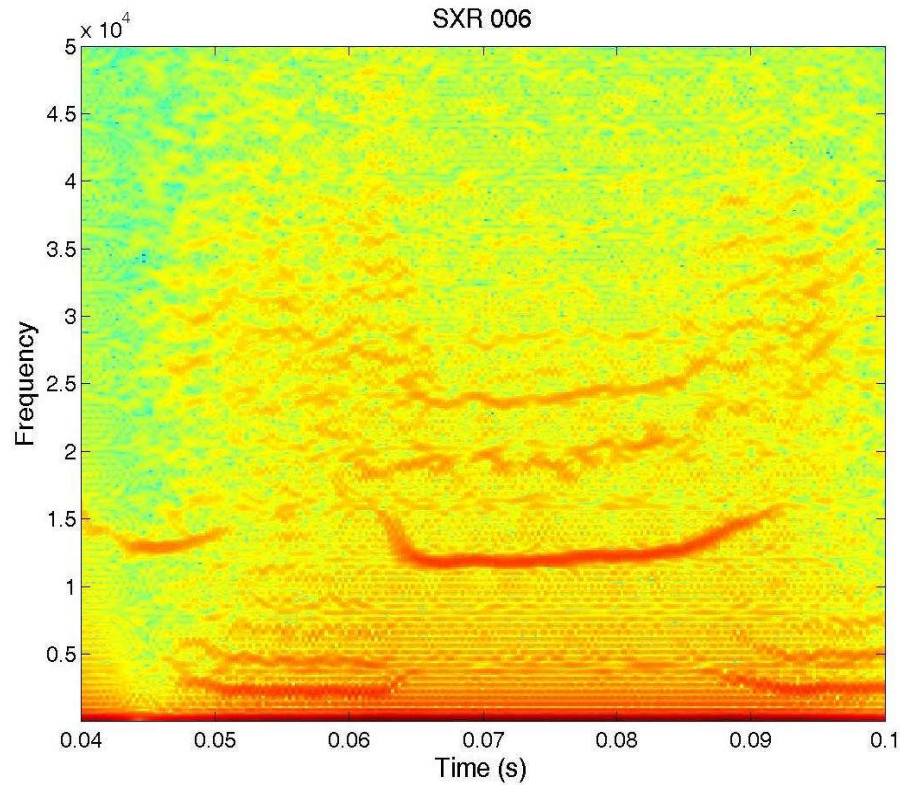
Fig. 8. Spectrogram of SXR- emission over line just 6mm outer of the magnetic axis in shot 23989.

The impurity accumulation in the plasma core can be explained as follows. Since the source of impurities is located outside the confined plasma, the abrupt increase of the electric field due to the externally imposed loop voltage rise or to the application of RF power at the plasma border may produce impurity, and generate inward impurity flux $\Gamma_I = -Z\Gamma_Z$ due to $D_i \gg D_e$. In the plasma region $1<q<2$, the impurities are mixed with hot core plasmas after each saw-tooth crash.

Then, the impurity core density will only depend on the ratio of the respective transport coefficients and the inward velocity v* and the diffusion coefficient D_Z. In neoclassical theory, we have v*/$D_Z \sim Z$, so that, the impurity will accumulate in the plasma core if the electron transport is not anomalous [12].

5. Conclusion

Experimental data obtained on TCABR confirm recent observations [1-5] of the amplification of the long distance correlations in potential fluctuations in the biasing H-mode, whereas correlation of density fluctuations is low. The significant LDC is already observable in the low confinement regime but LDC increases significantly at L-H transition. Together with these common features, there are distinct data on dominant components in V_f for the LDC. The LDC is caused by low frequencies $f < 20$-40 kHz without coherent modes in JT-II [1,3], while it is dominated by coherent mode ($f \sim 1.6$ kHz) in TEXTOR. Our data are more close to that of JT-II, i.e. the LDC is dominated by frequencies $f < 40$-60 kHz in our case. Under transition to biasing H-mode, the turbulent broadening in space of wavenumber k decreases substantially, and the coherent peaks of $S(k,f)$ spectrum have maximum values at $k \sim 0$.

We observed strong increase in the H-mode of very low frequency $f < 5$ kHz fluctuations and coherent peaks of fluctuations amplitude at the frequencies of around 15 kHz and 40 kHz.

Under transition to biasing H-mode, the turbulent broadening in space of wavenumber k decreases substantially, and the coherent peaks of $S(k,f)$ spectrum have maximum values at $k \sim 0$. The low frequency $f < 5$ kHz fluctuations with $k \sim 0$ is clear indication of zonal flows. The peak ~15 kHz may be caused by the low amplitude MHD instability with the same frequency measured by external magnetic probes. And the peak of amplitude at ~ 40 kHz may be considered as GAMs; while with measured, by Langmuir probes, electron temperature at the plasma edge ~30 eV, one have to expect in our case frequency $f_{GAM} \sim 15$ kHz.

The flattening of the electron temperature due to Alfvén wave heating or loop voltage rapid increment increases the inward impurity flux that helps the strong 2/1-tearing mode formation and, as a consequence, plasma core cooling.

Acknowledgements

References

[1] PEDROSA M.A., et al., Phys Rev. Lett., **100** 21503 (2008).
[2] SILVA, C., et al., Phys. Plasmas, **15** 120703 (2008).
[3] HIDALGO, C., et al., EPL, **87** 55002 (2009).
[4] XU, Y., et al., Phys. Plasmas, **16** 110704 (2009).
[5] MANZ, Y.P., RAMISCH, M., STROTH, U., Phys. Plasmas **16** 042309 (2009).
[6] MELNIKOV, A.V., et al., Plasma Phys. Control. Fusion, **48** S87 (2006)
[7] BESSON, G., et al., Plasma Phys. Control. Fusion, **28** SI 9A 1291 (1986)
[8] NASCIMENTO, I.C., et al., Nucl. Fusion, **45** 796 (2005).
[9] NASCIMENTO I.C., et al., Nucl. Fusion, **47** 1570 (2007).
[10] ALONSO, M.P., et al., Journal of Physics. Conference Series, v. 227, 012027 (2010).
[11] BELLINTINI, V., et al., 11th Latin American Workshop on Plasma Physics, DEC 05-09, 2006 Mexico City MEXICO, *Plasma and Fusion Science* 875, 350-356 (2006)
[12] DUX, R., Fusion Science and Technology, **44** 708 (2003).